Scanning tunnelling microscopy studies of β-amyloid fibril structure and assembly

A.P. Shivji[a], F. Brown[b], M.C. Davies[a], K.H. Jennings[c], C.J. Roberts[a], S.J.B. Tendler[a,*], M.J. Wilkinson[c], P.M. Williams[a]

[a]*Laboratory of Biophysics and Surface Analysis, Department of Pharmaceutical Sciences, The University of Nottingham, Nottingham, NG7 2RD, UK*
[b]*Molecular Neuropathology, Department of Neurosciences, SmithKline Beecham Pharmaceuticals, New Frontiers Science Park, Harlow, Essex, CM19 5AD, UK*
[c]*Microscopy and Flow Cytometry, Analytical Sciences Department, SmithKline Beecham Pharmaceuticals, Brockham Park, Betchworth, Surrey, RH3 7AJ, UK*

Received 27 June 1995

Abstract Alzheimer's disease is in part characterised by the deposit of β-amyloid peptide in the form of fibrils in the brain. In this study, the scanning tunnelling microscope (STM) has been used to provide high resolution images of synthetic fibril structure and formation as a function of time. Short fibrils are observed following brief peptide incubation times. At longer incubation periods ribbon like filaments were observed. These results suggest that β-amyloid self-assembly is an ordered process, with a correlation between time of incubation and length of β-amyloid filament growth.

Key words: Alzheimer's disease; β-Amyloid; Aggregation; Scanning tunnelling microscopy

1. Introduction

Alzheimer's disease is the major cause of dementia and the fourth leading cause of death in the developed world after heart disease, cancer and stroke. It has been estimated that it afflicts 10% of the population aged over 65 years [1,2]. The disease begins with the loss of short-term memory followed by progressive dementia [3]. A major pathological feature of Alzheimer's disease in the brain tissue of patients is the presence of a high density of amyloid plaques surrounded by neurons containing neurofibrillary tangles. Similar neuropathology is also evident in people with Down's Syndrome by their late thirties and appears also, in a reduced form, to be characteristic of the normal ageing process [4]. The amyloid of the plaques is composed of aggregations of β-amyloid peptide of 39–43 amino acid residues in length. The predominant peptide length depends on factors such as the type of plaque, its anatomical location, genotype and disease type. The β-amyloid peptide (1–40) sequence is shown in Fig. 1. β-Amyloid is derived from a transmembrane protein, amyloid precursor protein (APP), whose gene is located on chromosome 21 [5,6]. It is thought that abnormal post-translational modification of APP yields β-amyloid [7,8]. The neurotoxicity of β-amyloid is believed to be related to its self-assembly into long dense fibrils [9–13], which may act as cation-specific ion channels [14].

In an effort to understand the mechanism of molecular self-assembly we have studied the process of synthetic β-amyloid fibrilization using the scanning tunnelling microscope (STM). This instrument measures surface conductivity and is able to obtain topographical data in the nanometre to sub-nanometre range by monitoring the flow of current between a sharp probe and a surface [15]. In the last decade, the STM has found application in the fields of chemistry, physics, engineering and biology [16–18]. However, the poor electron conductivity of most biological samples has hampered the progress of direct imaging of macromolecules. To overcome this problem we have employed metal coating, which has the added benefit of physically immobilizing the sample [19]. Other potential protocols include chemical immobilization [20] or the use of high affinity binding systems [21].

The β-amyloid peptide is able to assemble in an aqueous environment [22–25]. In the present study we examine the effect of peptide incubation time on synthetic β-amyloid fibril structure and size. The samples, prepared for STM, allow a direct correlation of incubation time with structural elongation.

2. Materials and methods

2.1. Preparation of β-amyloid fibres

Synthetic β-amyloid (1–40) (Fig. 1) was obtained from Bachem (Torrance, California, USA). Samples were prepared to an initial stock solution concentration of 2 mg/ml using 0.1% acetic acid as the solvent. They were then stored at −20 °C to avoid fibrilization of amyloid. Self-assembly was initiated by dilution of stock solution to a concentration of 30 μg/ml (pH 4.5) by addition of the appropriate quantity of buffer. Aliquots of the sample were then incubated at 37°C for various time intervals.

2.2. Sample preparation

Immediately following dilution of the peptide and ageing, 4 μl of the respective solution was deposited onto freshly cleaved mica (Agar Scientific Ltd, Stansted, Essex, UK). The macromolecules were allowed to adsorb onto the substrate for a few minutes following which excess solvent was removed using filter paper. The samples were then dried rapidly under vacuum (10^{-6} T) and coated with a thin layer of platinum-carbon (nominally 2 nm thick as measured by a film thickness monitor) by electron beam evaporation in a Fisons E6430 coater [26]. The grain size obtained for coatings prepared in this way was approximately 4–5 nm as measured from STM images.

2.3. Microscope analysis

The samples were scanned in ambient conditions with mechanically prepared platinum/iridium (80:20) tips using a VG STM 2000 system (VG Microtech, Uckfield, UK). All the images shown were obtained in the constant current mode. Typical experimental conditions comprised a tunnelling current between 60 to 400 pA and a tip bias voltage range of +0.50 to +0.97 V. The images presented are grey scale representations, which show the lowest points as dark pixels and the highest points as light pixels. In order to establish the performance of the

*Corresponding author. Fax: (44) (115) 9515110.

SSDI 0014-5793(95)00858-6

instrument routine images of graphite were obtained at atomic resolution throughout the study.

2.4. Tip deconvolution

It is well known that scanning probe image data is often distorted by the geometric constraints imposed by the probe. Image data were analyzed using novel surface reconstruction software [27]. Here, the influence on the image of the shape of the bluntest tip that could have formed the image data is found and removed from the image surface. Features remaining in the image must, therefore, be representative of the smallest possible size of that surface feature. Such analysis permits the binding of width values; the upper bound is the width measured from the raw image data, the lower is that measured from the reconstructed surface. Data analysis indicates that fibril lengths are not significantly affected by tip geometric distortion. The software does not take into account the increase in dimensions due to the application of a metallic overcoat, however in our experience this does not tend to cause great deviation [20].

3. Results and discussion

STM analysis of the surface topography of the amyloid sample following minimal incubation revealed the self-assembled peptide, as shown in Fig. 2. The 188 × 188 nm scan is typical of similar data taken from a number of areas. The image shows a discrete surface unit which possesses a fibril-like structure. In addition, the fibril exhibits a corrugated sub-structure. Using similar high resolution scans, the dimensions of 40 filaments were measured. The mean length of the fibrils was 79.1 nm (standard deviation (S.D.) = 21.6). We believe these features to result from self-assembling of β-amyloid peptide. These amyloid assemblies may nucleate (or seed) the formation of larger insoluble aggregates of amyloid from pools of soluble peptide. While the exact nature of these structures is unknown, the net result of this so-called seeding phenomena is believed to be a significant acceleration in the rate of aggregation of β-amyloid compared with unseeded material [1,28].

It was evident from the STM data that increased self-assembly had occurred following incubation of the peptide for 4 h at 37°C. The 393 × 393 nm STM topograph (Fig. 3) is typical of data taken from a number of different areas within the prepared β-amyloid (1–40) peptide sample after 4 h. The image shows numerous discrete ribbon-like filaments on the surface which we again interpret to be self-assembled β-amyloid peptide [29,30]. Using higher resolution images, the dimensions of over 150 filaments were measured and again a heterogeneous size digstribution was obtained, with a mean length of 186.0 nm (S.D. = 59.6). A low percentage of very short fibrils of length around 20 nm were also clearly detected and we postulate that these are β-amyloid aggregates at an early stage of fibrilization.

There is a continued increased growth in plaque length at 24 h, as illustrated by the low resolution scan in Fig. 5 (1.9 × 1.9 μm). On analyzing the lengths of a large number of fibrils (n = 95), the mean length of the data was found to be 395.6 nm (S.D. = 144.9).

The STM image in Fig. 6, is typical of the sets of data recorded from a number of areas within the replicas analyzed following β-amyloid incubation for 216 h. The 1.8 × 1.8 μm

H_2N-Asp-Ala-Glu-Phe-Arg-His-Asp-Ser-Gly-Tyr-Glu-Val-His-His-Gln-Lys-Leu-Val-Phe-Phe-Ala-Glu-Asp-Val-Gly-Ser-Asn-Lys-Gly-Ala-Ile-Ile-Gly-Leu-Met-Val-Gly-Gly-Val-Val-COOH

Fig. 1. The β-amyloid (1–40) peptide sequence (the three letter code for amino acids has been utilized).

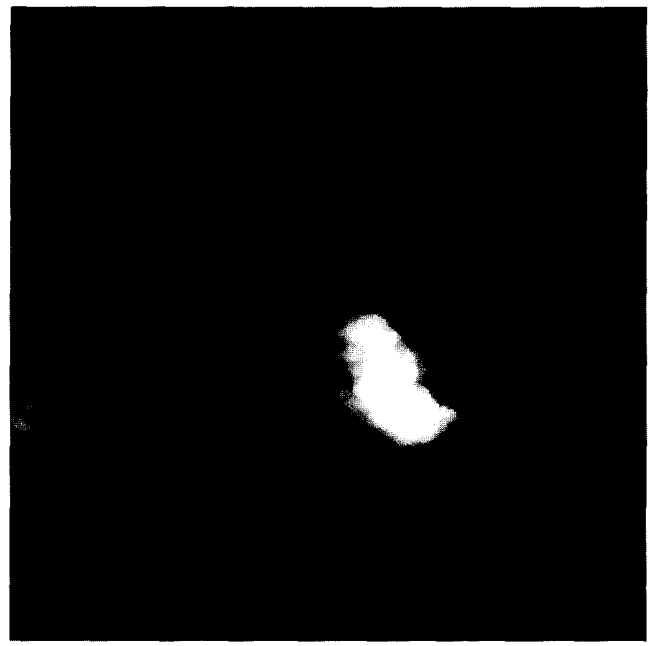

Fig. 2. STM image of coated samples prepared at t = 0 h. High resolution scan showing the distinct fibril morphology of β-amyloid. Scan size: 188 × 188 × 10.7 nm.

scan, shows a β-amyloid aggregate in the centre of the image. This single strand is flanked by a number of smaller surface units which we believe to be either smaller assemblies which may in time form larger self-assembled structures or debris as a result of long β-amyloid fibrils breaking up during the sample drying phase of the preparation. The high resolution topograph in Fig. 7 shows a number of long peptide aggregates which appear to exhibit a disjointed structure. This morphological

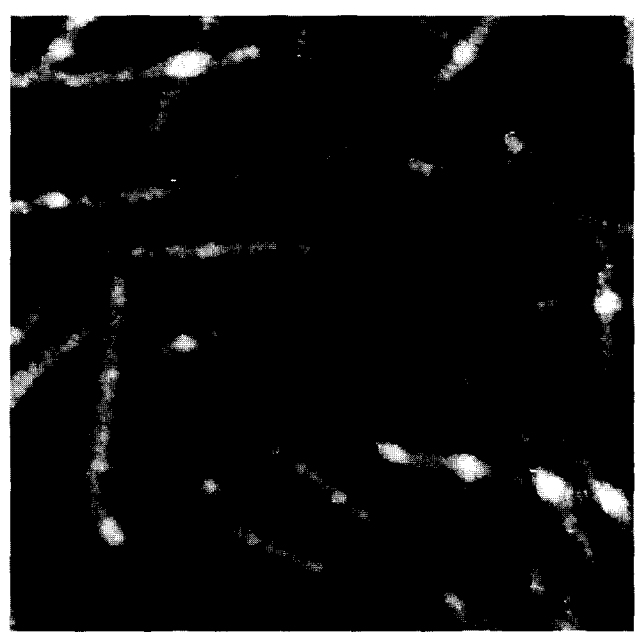

Fig. 3. STM image showing a number of discrete β-amyloid (1–40) surface units with a characteristic ribbon-like filament structure. Scan size: 393 × 393 × 11.5 nm. Coated samples prepared at t = 4 h.

Fig. 4. High resolution STM image of a single β-amyloid (1–40) fibril clearly exhibiting a striated morphology. Scan size 85 × 85 × 8.8 nm.

Fig. 6. Coated samples at $t = 216$ h. STM topographs of self-assembled ribbon like structures of β-amyloid (1–40) peptide. Scan size:1797 × 1797 × 40.8 nm.

feature is consistently repeated within a particular fibril, but differs between filaments. This variation in topography may be indicative of the angle of deposition of the fibril or represent the disruption involved caused by the drying processes. On analyzing the data, it was decided to eliminate any fibrils of length less than 750 nm, as aggregates of this length have been observed at 24 h and may be debris. The mean length of 39 fibres was found to be 1149.6 nm (S.D. = 301.4).

An analysis of the surface morphology also entailed an assessment of the width of the fibrils. In contrast to fibril length, the measurement of widths were more consistent for most of the self-assembled peptides and the average was found to be 25.3 nm (S.D. = 4.2). Using higher resolution images, similar to Fig. 4, it became evident the fibrils possessed a pronounced corrugated morphology (indicated with arrows). There appears to be a broad region followed by a narrower area, and on analysis it was found that this unit is repeated every 12 nm. This variation in width has been reported previously using transmis-

Fig. 5. STM image showing an apparent enlarging of the biomolecules length due to a self-assembling process, after incubation for 24 h. Scan size 1986 × 1986 × 19.6 nm.

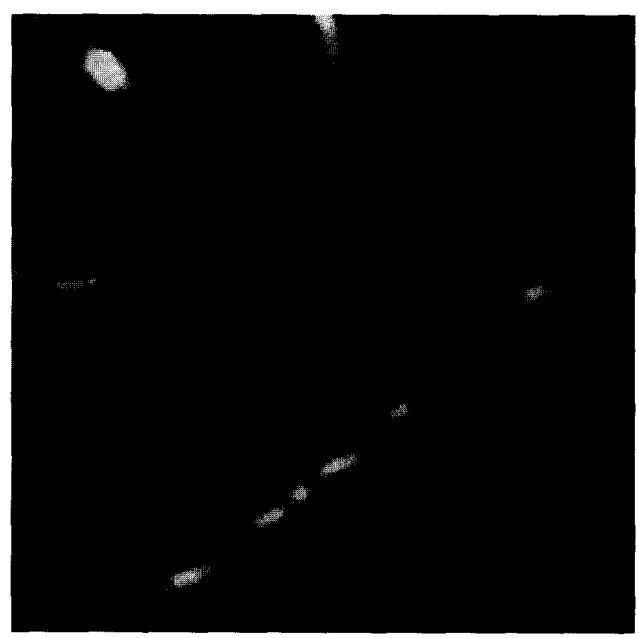

Fig. 7. Higher resolution scan showing disjointed structure of large fibrils. Scan size 530 × 530 × 25.1 nm.

Table 1
Analysis of mean dimensions of coated synthetic β-amyloid (1–40) peptide at various incubation times by STM

Mean length / nm at 0 h	Mean length / nm at 4 h	Mean length / nm at 24 h	Mean length / nm at 216 h	Mean width /nm*
79.1 ± 21.6	186.0 ± 59.6	395.6 ± 144.9	1149.6 ± 301.4	25.3 ± 4.2

*STM data shown here correlate well with TEM data (unpublished)

sion electron microscopy (TEM) [31]. An analysis of the tip induced effects indicated that the images obtained had not been distorted significantly by the probe and the features viewed were a true indication of the sample morphology. In addition, the STM data correlates well to data sets obtained with TEM, for samples prepared by coating with platinum-carbon [unpublished].

The experiments undertaken have produced high resolution data of β-amyloid fibrils. Initially small self-assembled rod shaped structures were observed. Following molecular self-assembly in solution a consistent ribbon like filament morphology was observed by STM. The surface topography was one of alternating areas of broad and slim regions within the amyloid structure. A summary of the data (Table 1) indicates a correlation between longitudinal fibre elongation, as determined by STM, and the time of incubation. Our results suggest that β-amyloid elongation is an ordered process in solution, with a quantifiable amount of fibril growth achievable in a set time.

Acknowledgements: A.P.S. gratefully acknowledges the provision of a BBSRC CASE Award with SmithKline Beecham Pharmaceuticals. P.M.W. is funded by a EPSRC/DTI Nanotechnology LINK Scheme in collaboration with Kodak Limited, Fisons Instruments and Oxford Molecular.

References

[1] Vitek, M.P., Bhattacharya, K., Glendening, J.M., Stopa, E., Vlassara, H., Bucala, R., Manogue K. and Cerami A. (1994) Proc. Natl. Acad. Sci. USA 91, 4766–4770.
[2] Scinto, L.F.M., Daffner, K.R., Dressler, D., Ransil, B.I., Rentz, D., Weintraub, S., Mesulam, M. and Potter, H. (1994) Science 266, 1051–1054.
[3] Hardy, J. and Allsop, D. (1991) Trends Pharmacol. Sci. 12, 383–388.
[4] Tanzi, R.E., St George-Hyslop, P.H. and Gusella, J.F. (1989) Trends Neurosci. 12, 152–158.
[5] Chun, M.R. and Mayeux, R. (1994) Curr. Opin. Neurol. 7, 299–304.
[6] Multhaup, G., Masters, C.L. and Beyreuther, K. (1993) Biol. Chem. 374, 1–8.
[7] Papastoitsis, G., Siman, R., Scott, R. and Abraham, C.R. (1994) Biochemistry 33, 192–199.
[8] Tanzi, R.E. (1989) Ann. Med. 21, 91–94.
[9] Mantyh, P.W., Ghilardi, J.R., Rogers, S., Demaster, E., Allen, C.J., Stimson, E.R. and Maggio, J.E. (1993) J. Neurochem. 61, 1171–1174.
[10] Buxbaum, J.D., Edward, K.H.I. and Greengard, P. (1993) Proc. Natl. Acad. Sci. USA 90, 9195–9198.
[11] Ueda, K., Fukui, Y. and Kageyama, H. (1994) Brain Res. 639, 240–244.
[12] Simmons, L.K., May, P.C., Tomaselli, K.J., Rydel, R.E., Fuson, K.S., Brigham, E.F., Wright, S., Lieberburg, I., Becker, G.W., Brems, D.N. and Li, W.Y. (1994) Mol. Pharm. 45, 373–379.
[13] Kirschner, D.A., Inouye, H., Duffy, L.K., Sinclair, A., Lind, M. and Selkoe, D.J. (1987) Proc. Natl. Acad. Sci. USA 84, 6953–6957.
[14] Arispe, N., Pollard, H.B. and Rojas, E. (1993) Proc. Natl. Acad. Sci. USA 90, 10573–10577.
[15] Binnig, G., Rohrer, H., Gerber, Ch. and Weibel, E. (1982) Phys. Rev. Lett. 49, 57–61.
[16] Rabe, J.P. and Bucholz, S. (1991) Phys. Rev. Lett. 66, 2096–2099.
[17] Hansma, P.K., Elings, V.B., Marti, O. and Bracker, C.E. (1988) Science 242, 209–216.
[18] Lindsay, S.M., Thundat, T. and Nagahara, L. (1988) J. Microscopy 152, 213–220.
[19] Leggett, G.J., Wilkins, M.J., Davies, M.C., Jackson, D.E., Roberts, C.J. and Tendler, S.J.B. (1993) Langmuir 9, 1115–1120.
[20] Leggett, G.J., Roberts, C.J., Williams, P.M., Davies, M.C., Jackson, D.E. and Tendler, S.J.B. (1993) Langmuir 9, 2356–2362.
[21] Lee, G.U., Kidwell, D.A. and Colton, R.J. (1994) Langmuir 10, 354–357.
[22] Schmechel, D.E., Saunders, A.M., Strittmatter, W.J., Crain, B.J., Hulette, C.M., Joo, S.H., Pericak-Vance, M.A., Goldgaber, D. and Roses, A.D. (1993) Proc. Natl. Acad. Sci. USA 90, 9649–9653.
[23] Kawahara, M., Muramoto, K., Kobayashi, K., Mori, H. and Kuroda, Y. (1994) Biochem. Biophys. Res. Commun. 198, 531–535.
[24] Tomiyama, T., Asano, S., Furiya, Y., Shirasawa, T., Endo, N. and Mori, H. (1994) J. Biol. Chem. 269, 10205–10208.
[25] Caputo, C.B., Sobel, I.R.E., Sygowski, L.A., Lampe, R.A. and Spreen, R.C. (1993) Arch. Biochem. Biophys. 306, 321–330.
[26] Wilkins, M.J., Davies, M.C., Jackson, D.E., Mitchell, J.R., Roberts, C.J., Stokke, B.T. and Tendler, S.J.B. (1992) Ultramicroscopy 48, 197–201.
[27] Roberts, C.J., Williams, P.M., Bestwick, C., Davies, J., Dawkes, A., Davies, M.C. and Tendler, S.J.B. (1995) Langmuir (in press).
[28] Harrington, C.R. and Colaco, C.A.L.S. (1994) Nature 370, 247–248.
[29] Fraser, P.E., Nguyen, J.T., Surewicz, W.K and Kirschner, D.A. (1991) Biophys. J. 60, 1190–1201.
[30] Gorevic, P.D., Castano, E.M., Sarma, R. and Frangiune, B. (1987) Biochem. Biophys. Res. Commun. 147, 854–862.
[31] Burdick, D., Soreghan, B., Kwon, M., Kosmoski, J., Knawer, M., Henschen, A., Yates, J., Cotman, C. and Glabe, C. (1992) J. Biol. Chem. 267, 546–554.